

INELASTIC ENERGY LOSSES IN GASES AND ELECTRONIC STOPPING POWERS IN SOLIDS

D. J. BIERMAN

FOM-Instituut voor Atoom- en Molecuulfysica, Amsterdam, Nederland

D. VAN VLIET

Department of Physics, Chalmers University of Technology, Gothenburg, Sweden

Received 28 May 1971

Synopsis

Inelastic energy-loss values have been measured from gas-phase collisions and are applied to derive values of the electronic stopping powers in solids using a computer simulation model. The specific cases investigated have been 19.4 keV Ne⁺ in copper, 21.0 keV Ne⁺ in nickel and 45.5 keV Ne⁺ in aluminium, both for random incidence and for perfect alignment along $\langle 001 \rangle$ or $\langle 101 \rangle$. These exploratory results indicate that the method is capable of providing realistic stopping-power values and, while probably less accurate than conventional techniques, should allow one to experimentally investigate the Z_1 and Z_2 oscillations in the stopping power and the transition in the stopping power from a channelled to a random trajectory from the point of view of single collisions.

The computer model has also been used to calculate penetration profiles for the above systems and allows one to study the relative energy deposition by both nuclear and electronic collisions. A “funelling” effect by which channelled orbits are consistently forced toward the centre of the channels has been observed in the $\langle 101 \rangle$ channels and leads to well-defined maximum ranges.

1. *Introduction.* The study of ion bombardment of solid targets has developed rapidly during the last few years, inspired in particular by the development of ion-implantation techniques for doping semiconductors. Questions of major research interest have centred on the radiation damage created by the implanted projectiles as they are brought to rest, their eventual depth beneath the surface and their final crystallographic position. The key to these problems lies in an understanding of the projectile orbits and the way in which they lose energy. The orbit is essentially controlled by elastic collisions with the target atoms, while the energy loss is normally divided into two distinct contributions¹): the energy lost to the target atoms (nuclear or elastic stopping) and the energy lost *via* the excitation of the electrons in either the target or the projectile itself (electronic or inelastic stopping).

In general the rate of energy loss may be expressed as an integral:

$$-\left(\frac{\partial E}{\partial Z}\right)_i = N \int \Delta E_i d\sigma(\Delta E_i), \quad (1)$$

where N is the atomic density of the target, ΔE_i is the energy lost in a single collision, and the subscript ‘‘ i ’’ refers to either electronic or nuclear processes. The usual method of treating nuclear stopping is to postulate an interatomic potential $V(r)$ between the projectile and target atoms, calculate ΔE_{nuc} as a function of the impact parameter s using classical scattering theory, and assume a random distribution of two-body collisions so that $d\sigma = 2\pi s ds$. This method cannot be applied when the distribution of collisions is no longer random but is somehow critically linked with the projectile orbits; *e.g.*, the well-known channelling effect where the projectile is confined to orbits near the centre of the open crystallographic channels and avoids all close collisions. Channelling results in a strong reduction in both the nuclear and electronic stopping powers.

An alternative method to derive stopping powers in a crystalline target is to apply computer simulation techniques to calculate the precise orbits of a large number of projectiles. By recording the elastic energy transfer in each successive collision one can derive a stopping power as averaged over all projectile orbits or, alternatively, over a particular set of orbits. The latter case could be applied to, say, channelling. The advantage of the computer simulation is that the crystallographic nature of the target is implicitly accounted for and effects such as channelling may be investigated in precise detail.

The electronic stopping, at least for heavy ions with an energy in the keV region as is the case with most implantation work, is primarily due to the excitation of bound electrons. The energy which can be transferred directly to the free electrons is small due to the large mass ratio. By treating the electrons as a degenerate electron gas Lindhard and Scharff²⁾ calculated a mean electronic stopping power valid at low velocities which was a monotonic function of Z_1 and Z_2 [†]. Experimental measurements of the transmission of ions through thin foils, however, have shown a remarkable oscillating behaviour in the electronic stopping power as a function of both Z_1 and, recently, Z_2 . To explain this phenomenon several authors³⁻⁷⁾ have modified a theory due to Firsov⁸⁾ which was originally developed to describe inelastic losses in two-body collisions of free particles. By making some assumptions, one of the most crucial being that one can describe bound electrons by the same wavefunctions both inside and outside the solid, one may derive mean electronic stopping powers. The correspondence between theory and ex-

[†] We adopt the standard convention whereby a subscript ‘1’ refers to the projectile and ‘2’ to the target atoms.

periment has proved to be surprisingly good and suggests that it should also be permissible to apply experimental values of inelastic losses derived from gas-phase collisions to the electronic stopping within a solid.

Small-angle scattering experiments in the FOM-institute for Atomic and Molecular Physics in Amsterdam have yielded inelastic energy losses as a function of the energy and distance of closest approach for two colliding atoms. These results have then been fed into a computer simulation program so that a specific inelastic loss is included in every elastic collision of the projectile. A mean electronic stopping power may be derived in exactly the same way as the mean nuclear stopping power. Alternatively, by following the projectiles until they come to rest the penetration depth and the various associated range distributions may be evaluated directly. The advantages of the computer techniques may therefore be applied to electronic losses as well as to the elastic.

2. *Inelastic energy losses during two-body collisions.* 2.1. Experimental procedure. A beam of ions accelerated to 60 keV is directed into a scattering chamber filled with a target gas at a low enough pressure to ensure single-collision conditions. A sputtering ion source enables one to bombard the gas atoms with ions from a solid; e.g., Al^+ , Ni^+ and Cu^+ . Primary ions scattering over small angles ($< 2^\circ$) are analyzed using a cylindrical electrostatic-energy analyzer with a resolution of 4×10^{-4} . An example of the recorded energy spectra is shown in fig. 1; the peak of the primary particles, $\theta = 0$, is used for calibration. The inelastic energy loss,

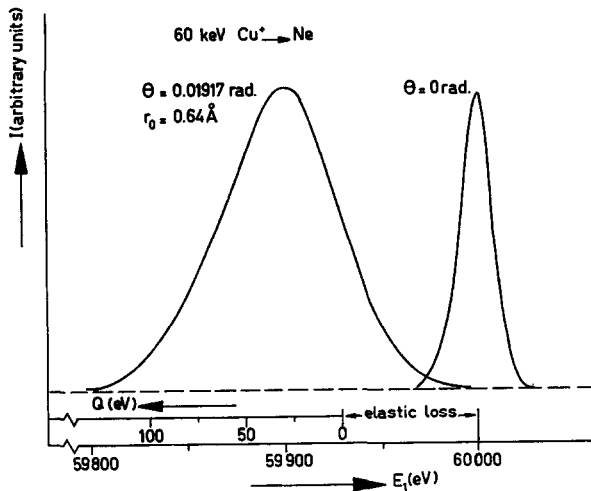


Fig. 1. An example of an energy spectrum of copper ions scattered over 0.01917 rad by neon. The energy distribution of the primary beam ($\theta = 0$) is used for calibration.

Q , is calculated from:

$$\frac{Q}{E_0} = \frac{2M_1}{M_2} \cos \theta \left(\frac{E_1}{E_0} \right)^{\frac{1}{2}} + \frac{M_2 - M_1}{M_2} - \frac{M_2 + M_1}{M_2} \frac{E_1}{E_0}, \quad (2)$$

where E_0 is the primary energy, E_1 is the secondary energy and θ is the scattering angle. A more detailed description of the experimental setup is given elsewhere⁹).

2.2. Experimental results. In any collision in which θ and E_0 are known the distance of closest approach, r_0 , may be determined from classical scattering theory once an interatomic potential has been postulated. In order to preserve the analogy with the Firsov theory and to facilitate introducing the results into the computer model we prefer to express Q as a function of r_0 . Figs. 2, 3 and 4 show the experimental results which were used in the computer calculations.

Experimentally, as may be seen from fig. 1, the width of the scattered peak is much greater than the width of the primary beam, so that the inelastic-energy loss does not have a unique value for a given value of r_0 . The total Q peak is thought to be composed of several closely spaced lines which are mostly unresolved due either to the finite resolution of the apparatus or a physical broadening of the lines. In cases where the structure can be resolved, *e.g.*, Al^+ on Ne, Q is determined as the weighted sum of the different lines. Thus fig. 2 shows the experimentally weighted \bar{Q} values as well as the elastic loss as calculated by the conservation laws. In the cases of 60 keV

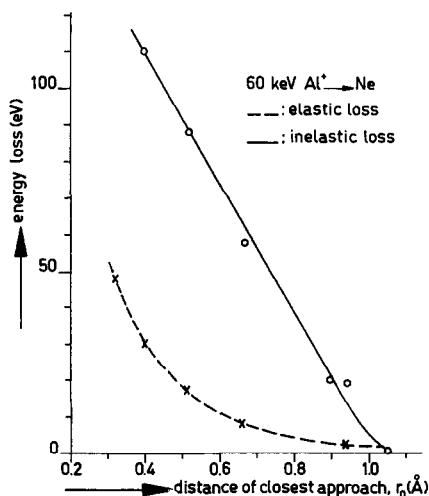


Fig. 2. The energy loss of 60 keV Al^+ ions scattered by neon as a function of the distance of closest approach. The elastic loss is calculated using the conservation laws of momentum and energy.

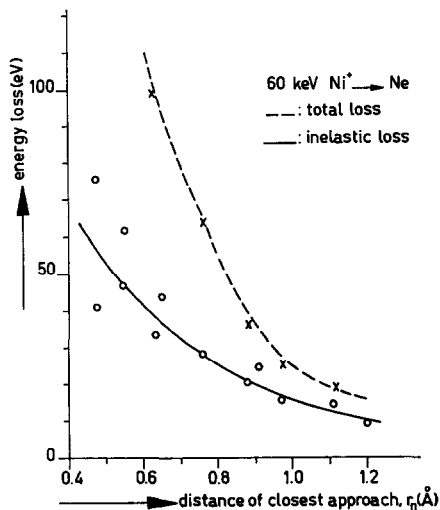


Fig. 3

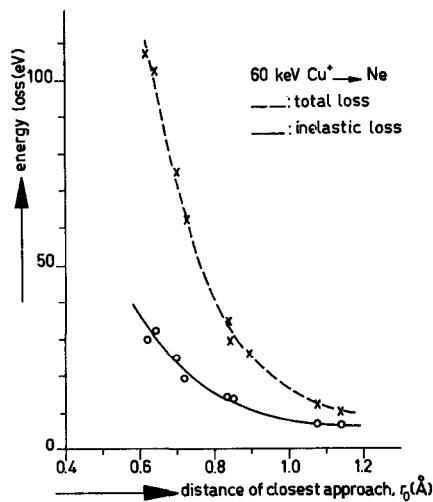


Fig. 4

Fig. 3. Energy-loss measurements of Ni^+ ions scattered by neon as a function of the distance of closest approach.

Fig. 4. Energy-loss measurements of Cu^+ ions scattered by neon as a function of the distance of closest approach.

Ni^+ and Cu^+ on Ne both the total energy loss ($E_0 - E_1$) and the mean inelastic loss \bar{Q} are plotted. To apply these results to the computer the following analytical fits to the experimental data were derived:

$$\text{Ar}^+ \rightarrow \text{Ne}: \quad \bar{Q} \approx \begin{cases} 184(1 - r_0) & r_0 < 1 \text{ \AA}, \\ 0 & r_0 > 1 \text{ \AA}, \end{cases} \quad (3)$$

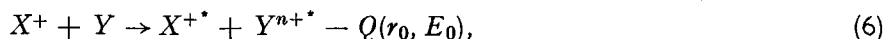
$$\text{Ni}^+ \rightarrow \text{Ne}: \quad \bar{Q} \approx 18/r_0^{1.5}, \quad (4)$$

$$\text{Cu}^+ \rightarrow \text{Ne}: \quad \bar{Q} \approx 11/r_0^2, \quad (5)$$

where \bar{Q} is in eV and r_0 in \AA .

We note from figs. 2, 3 and 4 that for Cu^+ and Ni^+ the elastic losses exceed the inelastic for $r_0 \lesssim 0.93$ and 0.83 \AA , respectively, while for Al^+ over the entire angular range of measurement the inelastic loss is larger than the elastic.

2.3. Application to solids. Several objections may be raised to applying the gas-phase results to solids. By electrostatically measuring the scattered primary ions we only observe processes in which the projectile remains ionized, *e.g.*:



but not those in which the final state contains the neutral projectile:

$$X^+ + Y \rightarrow X^* + Y^{n+*} - Q(r_0, E_0). \quad (7)$$

Moreover, the inelastic energy loss in a single collision goes into the excitation and/or ionization of either or both the target atom and the projectile. For r_0 of the order of 1 Å these involve mostly outer-shell processes. Since the state of the outer shell of energetic ions inside a solid is not well known but is likely to be an excited state and since the outer shell of the target atoms differs from that in the free state due to perturbations from the neighbouring atoms it is doubtful whether a collision in the solid with a velocity v and a distance of closest approach r_0 results in the same inelastic loss as an interaction in the gas with identical collision parameters.

Ideally to apply gas-collision results in a solid we should have the $Q(r_0, E_0)$ function which is the weighted mean over all the $Q_i(r_0, E_0)$ corresponding to the inelastic losses of projectiles in state “ i ”. We therefore require the equilibrium distribution of projectile states within the solid as well as more detailed gas collision experiments in which, for example, projectiles in different excited states are used. Furthermore our computer simulations will reverse the target and projectile and investigate the more common situation of Ne^+ ions incident on metallic targets of Al, Ni and Cu. According to the Firsov theory Q is only a function of r_0 and the relative velocity so that the inversion must be accompanied by a change of energy to $E'_0 = (M_2/M_1) E_0$. The appropriate values for $E_0 = 60$ keV are listed in table I. Experimentally¹⁴) there is evidence that this inversion is not strictly accurate but in the light of our assumptions it is not a critical failing.

On the positive side there are two points which appear to justify our procedure: first, the successes of the modified Firsov theory, which does not worry about these details, in predicting the observed oscillations in the electronic stopping power; and second, Snoek *et al.*¹⁵) have shown that the inelastic energy loss of projectiles scattered by surface atoms, whose electronic states are an intermediate case between free and bulk atoms, is the same as in the gas-phase collisions.

For these reasons the present calculations must only be regarded as exploring the possibilities of applying gas-phase collisions to interactions in solids; for the moment we only wish to determine whether or not the method is viable. If so it might be possible to explain some of the anomalies observed in the electronic stopping power, such as the Z_1 or Z_2 oscillations, by reference to gas-phase work. Furthermore it is of some interest to relate, even if only qualitatively, stopping powers and ranges with, say, the orientation of an external ion beam.

3. *Computer simulations.* 3.1. *The model.* The computer simulation model has been described in detail elsewhere^{16–18}). The elastic interaction

between the projectile and the target atoms is represented by the so-called Moliere approximation to the Thomas-Fermi potential:

$$V(r) = \frac{Z_1 Z_2 e^2}{r} (0.1 e^{-6r/a} + 0.55 e^{-1.2r/a} + 0.35 e^{-0.3r/a}), \quad (8)$$

where the screening radius $a = 0.47 (Z_1^{*3} + Z_2^{*3})^{-1/2} \text{ \AA}$. The orbits in the three-dimensional crystal are calculated with good precision by separating the interaction into a series of independent two-body collisions, the "binary approximation". With each collision we now include, in addition to the normal elastic energy loss, an inelastic energy loss Q as derived from the analytical fit to the experiments, (3) to (5). Thermal vibrations are introduced by allowing each target atom to vibrate independently about its equilibrium site.

3.2. Stopping powers. To calculate both the electronic and nuclear stopping powers a large number of ions are incident at random positions over a representative area of the crystal surface. Each projectile is followed down to a certain depth and the energy losses *via* elastic collisions and electronic excitation are both summed en route. The stopping power for each ion is defined as the total energy lost divided by the depth and the mean stopping powers are averaged over all incident ions. Since the ion trajectories are never straight lines, their total path length exceeds the penetration depth and our definition of a stopping power is in effect the rate of energy deposition along the beam direction. The results are independent of depth so long as the depth considered is long enough that some sort of equilibrium is attained (in the

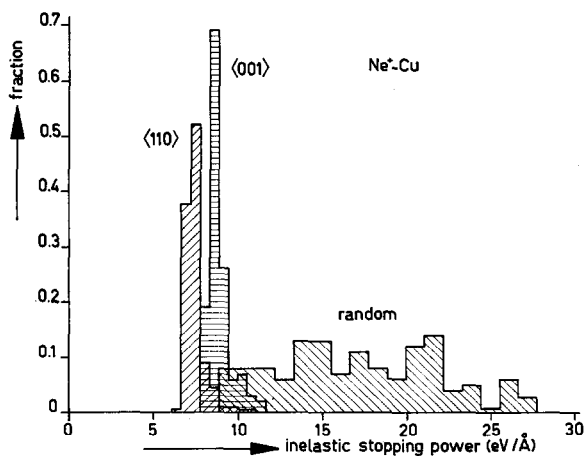


Fig. 5. Inelastic stopping-power distributions for 19.4 keV Ne^+ ions in copper given as the fraction of ions with an inelastic stopping power in a given energy interval. It can be seen, for example, that nearly all the ions directed into the $\langle 001 \rangle$ channel had an inelastic stopping power of 8 eV/Å.

case of channelled trajectories this means large compared to the "wavelength" of the orbits) and yet not deep enough to allow a significant change in the energy.

Fig. 5 shows the distribution in the electronic stopping power for 19.4 keV Ne^+ ions in copper, both for a non-crystallographic orientation and for perfect alignment with the $\langle 001 \rangle$ and $\langle 101 \rangle$ channels. The distributions in the latter cases only include the channelled ions since there is also a high-energy loss tail corresponding to that small fraction of the beam which lands near an atomic row and is dechannelled. The width of the random peak is essentially statistical and over larger depths would become narrower. The relatively narrow spread of the channelled losses corresponds to variations in the stopping power from different channelled orbits. Ions of different transverse energy sample different distributions of impact parameters and hence lose energy at different rates. The sharp peak implies that the stopping power is not very sensitive to multiple-scattering effects which change the distribution of transverse energy. We have already noted from fig. 1 that there is a spread of Q values in any collision which, since we assume a unique relationship between Q and r_0 , is missing from our simulations. In all three cases investigated, the full width at half maximum of this spread reaches values of up to 80% of the \bar{Q} value⁹⁾ and therefore exceeds greatly the orbital spread.

Table I summarizes the mean electronic stopping powers obtained for Ne^+ in Al, Ni and Cu. The channelled results are consistently lower than the random results; the fractional reduction varies from 85% to 35% so that no one single rule is evident. The stopping powers are lower in the more

TABLE I

Electronic stopping powers for Ne^+ (eV/Å)				
E'_0	Crystal	$\langle 101 \rangle$	$\langle 001 \rangle$	Random
45.5 keV	Al	2.2	3.6 ₅	14.4
21.0	Ni	14.5	16.1	25.1
19.4	Cu	7.4	9.1	18.7

TABLE II

Nuclear stopping powers for Ne^+ (eV/Å)			
Crystal	$\langle 101 \rangle$	$\langle 001 \rangle$	Random
Al	0.36	0.69	28
Ni	1.37	2.1 ₅	70
Cu	0.68	2.5	54

open $\langle 101 \rangle$ channels than in $\langle 001 \rangle$, as one would expect from the decrease in Q with increasing r_0 . Table II lists the comparable nuclear stopping powers, and now variations by factors of almost 100 are found between the random and channelled data. For a random orientation the nuclear stopping power at these energies exceeds the electronic by a factor of 2 to 3 but in the channelled cases it is generally an order of magnitude smaller. This is due to the fact that ΔE_{nucel} is far more sensitive to s than is Q ; in the limit of large impact parameter s for the Moliere potential (8), $\Delta E_{\text{nucel}} \propto e^{-0.6s/a}$. The distribution of nuclear stopping powers, not plotted, is correspondingly much wider.

The channelled results may be compared with the minimum possible stopping powers that would apply to a best-channelled ion moving perfectly

TABLE III

Crystal	Minimum channelled stopping powers for Ne^+ ($\text{eV}/\text{\AA}$)			
	Electronic		Nuclear	
	$\langle 101 \rangle$	$\langle 001 \rangle$	$\langle 101 \rangle$	$\langle 001 \rangle$
Al	0	0	0.036	0.050
Ni	11.6	14.8	0.25	0.36
Cu	5.4	7.6	0.23	0.37

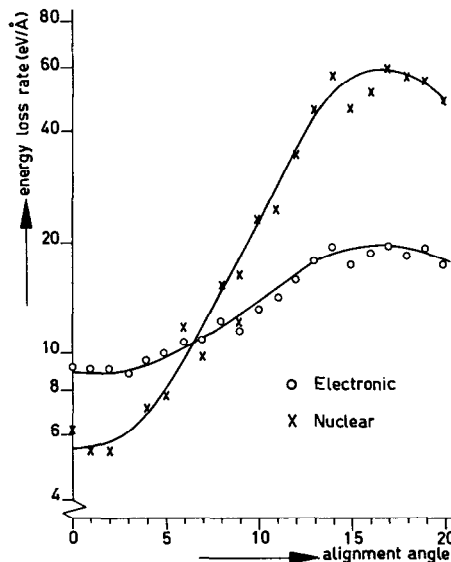


Fig. 6. The variation of the mean electronic and nuclear stopping powers for 19.4 keV Ne^+ ions in copper as a function of the angle of alignment, ψ_{1n} , relative to $\langle 101 \rangle$. The lattice temperature was 0°C .

down the mid-channel axis. The latter have been listed in table III. In the Cu and Ni channels the mean electronic stopping powers are only about 25% greater than the minimum; in aluminium the channel radii exceed the largest value of r_0 for which inelastic losses could be detected experimentally but a zero-energy loss rate is no doubt physically unrealistic. The minimum nuclear stopping power is considerably less than the mean for the reasons stated above.

Fig. 6 illustrates the variation in the mean (*i.e.* averaged over both channelled and non-channelled orbits) stopping powers for 19.4 keV Ne^+ ions in copper as a function of the alignment angle relative to $\langle 101 \rangle$. Once again the electronic stopping is relatively insensitive to slight misorientations while the nuclear stopping is far more sensitive and shows a larger total variation. The absence of a pronounced shoulder, in particular for the electronic case, is due to the fact that the total stopping power is not exclusively controlled by very low impact parameter collisions (which would show a more pronounced shoulder) but is also sensitive to the more frequent large impact parameter collisions. The angular half-widths are quite close to the Lindhard¹⁹⁾ characteristic angle ψ_2 ; in this case 9.0° .

TABLE IV

Random electronic stopping powers for Ne^+ (eV/Å)				
E_0'	Crystal	Computed	Lindhard and Scharff ²⁾	Experimental ¹⁴⁾
45.5 keV	Al	14.4	20.2	18.5
21.0	Ni	25.1	28.0	—
19.4	Cu	18.7	25.6	—

Table IV compares the random electronic stopping powers with the Lindhard and Scharff²⁾ formula and also with the one available experimental result of Ormrod *et al.*¹⁴⁾ for Ne^+ in Al. The results for both Al and Cu are significantly lower than the Lindhard values and the single experiment while the nickel result is much closer. It must be stressed, however, that the random results are not expected to be particularly accurate. For example it is probably not valid to extrapolate the experimental results back to high- Q , low- r_0 collisions which can be essential in determining the random stopping power. (This objection does not apply to channelled stopping powers.) Furthermore in the computer model we somewhat arbitrarily set an upper limit of one half the lattice parameter to the impact parameters considered; increasing this cutoff could artificially bring the results more into line with the Lindhard formula. This just illustrates how sensitive in fact our "quantitative" results are to the assumptions made in the model.

Since the inelastic losses have only been calculated at one energy we

cannot attach an energy dependence to our results. However, both the theoretical models of Firsov⁸⁾ and Lindhard and Scharff²⁾ give an $E^{\frac{1}{2}}$ dependence for the electronic stopping power so that it does not seem totally inappropriate to multiply the Q values given in (3), (4) and (5) by a factor $(E/E_0)^{\frac{1}{2}}$. We shall make use of this approximation in deriving ranges. From the momentum approximation we know that the channelled nuclear stopping powers go as E^{-1} ; no energy dependence has been worked out for the random nuclear stopping power.

3.3. Ranges. In the regime of projectile masses and energy that we are concerned with it is more common and of more direct application to measure the penetration of the implanted ions rather than their mean stopping power. We have extended our computations to calculate range profiles with the assumption that the inelastic losses obey an $E^{\frac{1}{2}}$ relationship as mentioned above. Starting with a large number of randomly positioned ions on the entrance surface, as above, each ion is followed until its energy drops low enough that it should be trapped within the crystal. We have somewhat arbitrarily taken 1 keV as the lower energy limit since the binary collision model starts to become unreliable at lower energies and the residual range at 1 keV should be comparatively small.

The range profiles obtained for 19 keV Ne^+ ions in copper for a number of different orientations are plotted in fig. 7 as integral distributions, *i.e.* the fraction of ions not yet stopped after a given depth measured parallel to the beam direction. The random profile corresponds to an incident

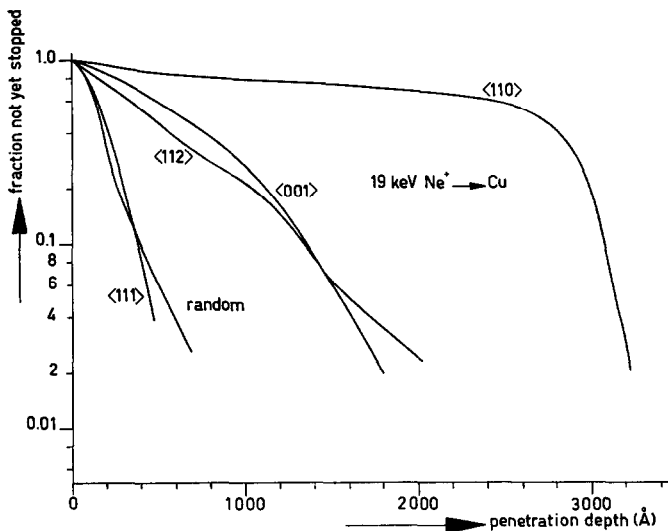


Fig. 7. Range profiles of 19 keV Ne^+ in copper for different orientations. The lattice temperature is 0°C . Perfect alignment is assumed.

direction well off any low-index row or plane. The lattice temperature was 0°C and we have assumed perfect beam collimation.

It is quite evident that the aligned beams have distinctly longer penetration depths than the random orientation, due primarily to the almost complete absence of nuclear stopping and to a lesser extent by the reduction in electronic stopping. Such an effect is of course well known both from experiments and theory. Thus there is a strong qualitative resemblance between our profiles and those measured experimentally in a number of f.c.c. metals²⁰⁾, as well as to those obtained by Robinson and Oen²¹⁾ for 5 keV Cu ions in Cu using a computer simulation model in which only the nuclear stopping was considered. There is therefore no startling effect due to the introduction of inelastic losses that are sensitive to the impact parameter.

Two particular points of interest might be mentioned:

(1) A very well-defined maximum range is found in the $\langle 101 \rangle$ channels but not in either $\langle 001 \rangle$ or $\langle 112 \rangle$, the next most open channels. This is caused by some process which consistently tends to focus or "funnel" a large fraction of the ions toward the centre of the channel where they experience a constant and minimal stopping power. This funnelling effect has only been observed in the $\langle 101 \rangle$ channels. The effect is further illustrated in fig. 8 which illustrates the flux of ions (relative to the flux at the incident surface) found near the mid-channel axis as a function of depth in both $\langle 101 \rangle$ and $\langle 001 \rangle$ channels. The centre of any channel normally samples a higher than normal flux since it is accessible to all channelled ions whereas positions near the atomic strings are only accessible to those ions of high transverse energy. The resultant variation in flux is known as flux peaking²²⁾. In the $\langle 001 \rangle$ channels multiple scattering tends to increase the transverse energy such that the accessible area for each ion also increases and the central flux

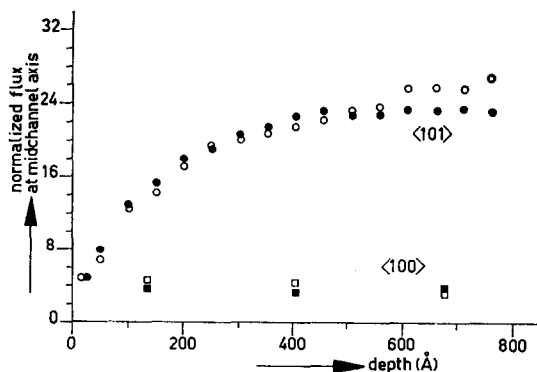


Fig. 8. The normalized flux at the mid-channel axis in different channels for 19 keV Ne^+ on copper. The central flux in the $\langle 101 \rangle$ channel increases with depth due to the funnelling effect.

decreases with depth. The range in this case is essentially determined by how long the ions can remain in their preferential orbits before being de-channelled. On the other hand the central flux in the $\langle 101 \rangle$ channels increases with depth as funnelling accentuates the normal flux peaking until it can reach a value of almost 25 times normal. The origin of the effect has not yet been discovered. It is not, however, the "damping" effect mentioned by Lindhard¹⁹⁾ by which the electronic stopping reduces both the total energy and the transverse energy proportionately. Thus in fig. 8 the open points were obtained with no inelastic losses; the solid points, with the inelastic loss (5) included. Within the expected statistical errors, of the order of 10%, no significant difference is found between the two. It is therefore evident that funnelling is somehow associated with the elastic collisions but it does not seem possible to explain it by involving the usual continuum approximation. For example the maximum flux accumulates not at the point of minimum continuum potential energy in the $\langle 101 \rangle$ channel but at its geometric centre, the point of intersection of the (010) and (10 $\bar{1}$) atomic planes. Since the channel is diamond shaped the positions of minimum average potential energy are displaced from the centre along the long $\langle 10\bar{1} \rangle$ axis. The importance of a funnelling effect, if confirmed, for penetration studies is obvious.

TABLE V

Total energy dissipated by 19 keV Ne ⁺ ions slowing down to 1 keV in copper (in keV)				
Orientation	Electronic	Total	Nuclear	
			$\Delta E_{\text{nuc}} > 20 \text{ eV}$	$\Delta E_{\text{nuc}} < 20 \text{ eV}$
Random	3.0	15.0	14.6	0.42
$\langle 111 \rangle$	3.4	14.6	14.1	0.47
$\langle 112 \rangle$	5.1	12.9	12.1	0.82
$\langle 001 \rangle$	5.8	12.2	11.1	1.1
$\langle 110 \rangle$	11.3	6.7	4.6	2.1

(2) The mean energy dissipated by 19 keV Ne⁺ slowing down to less than 1 keV in copper in both electronic and nuclear processes is listed in table V for the five orientations tested. In all cases except $\langle 101 \rangle$ the energy has gone predominantly to the target atoms *via* nuclear collisions, largely independent of the orientation. The elastic energy transfers may be further analyzed in terms of those above and below 20 eV, corresponding roughly to the transition from displacement to non-displacement knock-ons. According to the simplest models of atomic displacement cascades the number of displaced atoms should be directly proportional to the energy transferred in knock-ons above the displacement threshold. These results

indicate that despite the large differences in range there is a much smaller change in the number of displaced atoms in going from a random orientation to all channelled orientations except $\langle 110 \rangle$. Due to the above-mentioned funnelling effect the latter shows an approximately threefold reduction.

On the other hand there are significant changes in the energy distribution of the primary knock-ons if not in the total energy. The channelled orientations show a strong preference for low-energy transfers as witnessed by the significant increases in the sub-threshold losses. It is therefore not unreasonable to expect that the eventual damage state would differ considerably between a channelled and a random orientation. For example, recent work²³⁾ on the damage produced at ion irradiated copper surfaces indicated that surfaces are damaged through knock-ons with energies between 9 and 36 eV, which can initiate focussed collision sequences directed towards the surface.

Preliminary results for Ne^+ in Ni are qualitatively similar to those in Cu. So too are the Al results with the one exception that the combination of funnelling along $\langle 101 \rangle$ and the zero minimum electronic stopping power (see table III) leads to inordinately long $\langle 101 \rangle$ ranges. Although the experimental results showed that the inelastic losses for aluminium exceed the elastic ones for large impact parameters, the total energy losses are obviously dominated by the relatively infrequent large-angle scattering events where the nuclear losses are greater; hence the total energy lost *via* nuclear collisions exceeds that due to electronic collisions in this case as well.

4. *Conclusions.* The calculation of an inelastic energy loss in addition to the normal elastic loss for each individual collision is more consistent with the use of computer simulations to study ion bombardment of solids than the introduction of a mean electronic stopping power to account for the inelasticity of the collision processes. However, as we have already stressed the present series of calculations must be viewed as exploratory. At this point it does appear that the application of inelastic energy losses obtained from gas-gas scattering experiments to the derivation of electronic stopping powers in solids yields reasonable, if somewhat low, values. We would certainly not claim that the method could be made more accurate than conventional techniques; nevertheless, it does offer one or two interesting possibilities for qualitative studies, *e.g.* the Z_1 and Z_2 oscillations in the electronic stopping power in terms of individual collisions, or the relationship between the electronic stopping power and the orbits. Qualitatively the following conclusions may be drawn from the computations:

- (1) The ratio of the channelled electronic stopping power to that in a random medium can vary considerably from channel to channel or from one atom-ion system to another.
- (2) The variation in electronic stopping powers over individual channelled trajectories is small compared to the mean so long as the inherent width

of the inelastic loss per collision is not included. For this reason the mean electronic stopping is insensitive to, say, multiple scattering or slight misorientations.

- (3) The reduction in the mean nuclear stopping power for channelled alignment as well as the variation over individual trajectories are significantly greater than in the electronic case.
- (4) The relative penetration along different channels is not altered qualitatively by introducing an impact-parameter sensitive inelastic loss in addition to the nuclear loss.
- (5) An anomalous effect, termed "funnelling", in the $\langle 101 \rangle$ channels accentuates the flux-peaking behaviour and leads to a well-defined maximum range. The reason for this phenomenon might be found in reduction of the mean transverse energy due to breaking down of the continuum potential model for $\langle 101 \rangle$ strings. Indeed, computer simulations of reflection of ions at glancing incidence on surface strings²⁴) show cases in which the mean reflection angle is smaller than the mirror reflection angle.
- (6) Despite the sensitivity of the range profile to orientation, the distribution of the total deposited energy into nuclear and electronic components is much less sensitive to orientation. There is, however, a marked enhancement of low-energy elastic transfers for channelled orientations.

Acknowledgements. We want to thank Mr. W. C. Turkenburg for his assistance in the acquisition of the experimental data and the Physics Department of Chalmers University of Technology for offering the opportunity to do the computer calculations. This work is part of the research program of the Stichting voor Fundamenteel Onderzoek der Materie (Foundation for Fundamental Research on Matter) and was made possible by financial support from the Nederlandse Organisatie voor Zuiver Wetenschappelijk Onderzoek (Netherlands Organization for the Advancement of Pure Research).

REFERENCES

- 1) Bohr, N., *Mat.-fys. Medd. Danske Vidensk. Selsk.* **18** (1948) 8.
- 2) Lindhard, J. and Scharff, M., *Phys. Rev.* **124** (1961) 128.
- 3) Bhalla, C. P. and Bradford, J. N., *Phys. Letters* **27A** (1968) 318.
- 4) Winterbon, K. B., *Canad. J. Phys.* **46** (1968) 2429.
- 5) Cheshire, I. M., Dearnaley, G. and Poate, J. M., *Phys. Letters* **27A** (1968) 304.
- 6) Cheshire, I. M. and Poate, J. M., *Proc. Int. Conf. At. Coll. Phen. in Solids*, Brighton (1969).
- 7) Bhalla, C. P. Bradford, J. N. and Reese, G., *Proc. Int. Conf. At. Coll. Phen. in Solids*, Brighton (1969).
- 8) Firsov, O. B., *Zh. eksper. teor. Fiz.* **36** (1959) 1517.

- 9) Bierman, D. J., Bhalla, C. P. and Turkenburg, W. C., to be published in *Physica*.
- 10) Fastrup, B., Hermann, G. and Smith, K. J., to be published in *Phys. Rev.*
- 11) Barat, M., Baudon, J., Abignoli, M. and Houver, J. C., *J. Phys. B.* **3** (1970) 230.
- 12) Bierman, D. J. and Turkenburg, W. C., *Phys. Rev. Letters* **25** (1970) 633.
- 13) Bierman, D. J. and Turkenburg, W. C., to be published in *Physica*.
- 14) Ormrod, J. H., MacDonald, J. R. and Duckworth, H. E., *Canad. J. Phys.* **43** (1965) 275.
- 15) Snoek, C., Van der Weg, W. F., Geballe, R. and Rol, P. K., *Physica* **35** (1967) 1.
- 16) Morgan, D. V. and Van Vliet, D., *Canad. J. Phys.* **46** (1968) 503.
- 17) Morgan, D. V. and Van Vliet, D., Harwell Report AERE R 6283 (1970).
- 18) Van Vliet, D., *Computer Studies of Channelling in Crystals*, to be published in "Studies in Radiation Effects", Gordon and Breach (New York, 1971).
- 19) Lindhard, J., *K. Danske Vidensk. Selsk. mat.-fys. Medd.* **34** (1965) 14.
- 20) See, for example, Nelson, R. S., *The Observation of Atomic Collisions in Crystalline Solids*, North-Holland Publishing Co. (Amsterdam, 1968).
- 21) Robinson, M. T. and Oen, O. S., *Phys. Rev.* **132** (1963) 2385.
- 22) Van Vliet, D., to be published in *Radiation Effects*.
- 23) Elich, J. J. Ph., Roosendaal, H. E., Kersten, H. H., Onderdelinden, D., Kistemaker, J. and Elen, J. D., to be published in *Radiation Effects*.
- 24) Parilis, E. S., Turaev, N. Yu, Kivilis, V. M., IX Int. Conf. on Phen. in Ion. Gases, Bucharest (1969) contribution 2.2.2.5.